Chapter 2

A Highly Stable and Efficient Quasi-Solid-State Dye Sensitized Solar Cell Based on Poly(methyl methacrylate)/Polyaniline Nanotube Gel Electrolyte

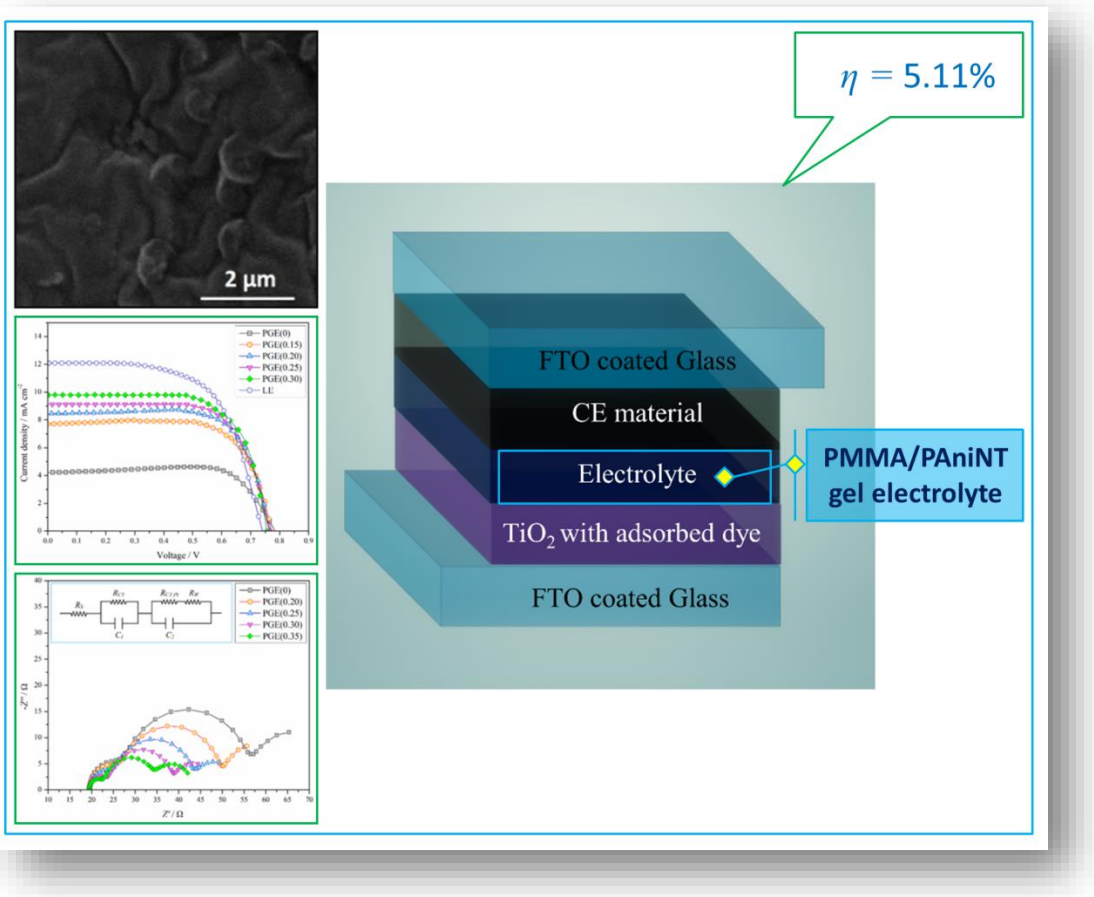

DSSC based on PMMA/PAniNT blend PGE gives an efficiency of 5.11%, wherein PAniNT helps in improving the ionic conductivity of the gel electrolyte to increase the magnitude of J_{SC}.

2.1 Introduction

Since the first demonstration by M. Grätzel and B. O'Regan in 1991, dye sensitized solar cells (DSSCs) have attracted a significant attention in the following years because of their high photoelectric conversion efficiency, easy fabrication technique and low cost [1–3]. DSSCs have a great potential to become the next generation solar cell. They are constructed by using a wide band-gap mesoporous semiconductor with adsorbed dye molecules where the dye molecules play the role of the sensitizer. On irradiation with light of specific wavelength, the photoexcited electrons of the dye molecules are injected into the conduction band of the semiconductor (e.g., titanium dioxide, TiO_2). A redox couple is present in the cell which reduces the oxidized dye molecules back to its original state. Usually, an iodide/triiodide (I^-/I_3^-) redox couple in an organic solvent comprises the liquid electrolyte. At the platinum (Pt) counter electrode, the I_3^- ions are reduced to I^- ions, resulting in countable amount of electric current [4–6]. Although highly efficient liquid electrolyte based DSSCs have good light-to-electric conversion efficiency, the durability of such cells is questionable due to leakage and evaporation of the solvents [7,8]. Many attempts have been made to replace the liquid electrolyte by solid polymer electrolytes, organic hole transfer materials, room temperature ionic liquids and gel electrolytes for improving the durability along with good efficiency [9–14]. Amongst them, polymer gel electrolytes (PGEs) have become the most promising candidates as they exhibit high ionic conductivity, durability and excellent interfacial properties at the electrodes [15,16]. Thus without compromising the photoconversion efficiency and long-term stability, liquid electrolyte can be replaced by PGE. Various polymeric materials are used as the polymer host to prepare the gel electrolytes [17–22].

Wu et al. reported a novel DSSC employing poly(ethylene glycol) (PEG) gel electrolyte consisting of potassium iodide (KI) and iodine (I_2) redox couple in propylene carbonate [23]. In another work, the same group reported a novel polymer blend electrolyte of polyvinylpyrrolidone (PVP) and PEG for DSSCs [24]. Hsu et al. introduced a graphene oxide nanosheet (GOS)-polyaniline (PAni) nanohybrid/poly(ethylene oxide)(PEO) blend gel electrolyte with good ionic

---

This part of the thesis is published in:

Mohan, K., Bora, A., Nath, B. C., Gogoi, P., Saikia, B.J., and Dolui, S. K. A highly stable and efficient quasi solid state dye sensitized solar cell based on Polymethyl methacrylate (PMMA)/Polyaniline Nanotube (PANI-NT) gel electrolyte. *Electrochimica Acta*, 222:1072-1078, 2016.

conductivity and efficiency [25]. Aram et al. have reported a novel quasi-solid-state DSSC with 4.9% photoconversion efficiency using poly(methyl methacrylate) (PMMA) blend with PEO polymer host with good interfacial properties between the gel electrolyte and the electrodes [26].

Good interfacial adhesion between the electrodes and the gel electrolyte is essential for good cell performance [27]. Efficient interfacial contact with the electrodes can be achieved by using amorphous thermoplastic polymer host as the gel electrolyte. In this regard, amorphous, transparent and colorless thermoplastic PMMA is a convenient candidate as a polymer host [26]. It has the ability to form a stable gel electrolyte with proper solvent mixture. In this work, we have chosen PMMA as the polymer host to prepare the gel electrolyte.

The charge transfer kinetics can be improved by introducing various conductive polymers into the polymer matrix. Among the different conductive polymers, polyaniline nanotubes (PAniNTs) have immense potential to improve the ionic conductivity of polymer based gel electrolyte [28,29].

In the present study, PMMA based PGE is used for fabrication of DSSC. Different weight percentages (wt%) of PAniNT is used to optimize the current density of the gel electrolyte. The ionic conductivities of the gel electrolytes are measured, and the cell performances of the novel quasi-solid-state DSSCs are studied from their current density-voltage (*J*-*V*) characteristics.

2.2 Experimental

2.2.1 Materials

Methyl methacrylate (MMA) was purchased from Himedia. TiO_2, benzoyl peroxide (BPO), lithium iodide (LiI), 4-tert-butylpyridine (TBP), 1-propyl-3-methylimidazolium iodide (MPI), N-methyl 2-pyrrolidone (NMP), cis-bis(isothiocyanato)bis(2,2′-bipyridyl-4,4′-dicarboxylate) ruthenium(II) bis-tetrabutylammonium (N719), titanium tetrachloride ($TiCl_4$) and chloroplatinic acid (H_2PtCl_6) were purchased from Aldrich. I_2, aniline, diethyl ether, methanol, oxalic acid, ammonium persulfate (APS), acetonitrile, acetone, isopropanol and sodium borohydride ($NaBH_4$) were purchased from Merck Millipore. All the reagents were used without any further purification. Fluorine doped tin oxide (FTO) coated conducting glass plates, sheet resistance 15 Ω cm^{-2} were also procured from Sigma Aldrich.

2.2.2 Synthesis of poly(methyl methacrylate)

PMMA was synthesized by free radical polymerization of the monomer, MMA. Briefly, MMA (10 mL) was taken in a 100 mL three-neck round-bottom (RB) flask equipped with a

magnetic stirrer, a nitrogen inlet and a thermometer pocket. BPO (0.1 g) was then added to the RB flask maintaining nitrogen (N_2) environment. The stirring was maintained at 1000 rpm and the temperature was raised to 70°C. The process was continued until the mixture turned into a viscous liquid. The viscous liquid was then poured into a petri dish and kept at 40 °C for one day to get transparent colorless PMMA. PMMA was then purified by re-precipitation in ethanol.

2.2.3 Synthesis of polyaniline nanotubes

To synthesize PAniNT, 0.5 mmol oxalic acid and 2 mmol aniline were dissolved in 10 mL of distilled water in an RB flask. The mixture was then cooled down to 4ºC. 5 mL of 2 mmol aqueous solution of APS was then poured into the RB flask slowly under vigorous stirring. The dispersion was then kept undisturbed for 12 h at 4ºC [30]. The resulting product was washed with distilled water, methanol and diethyl ether followed by drying at room temperature under vacuum to get PAniNT nanoparticles.

2.2.4 Synthesis of PMMA/PAniNT based polymer gel electrolytes

A series of PGEs were synthesized using PMMA/PAniNT polymer blends. The blends were prepared by adding different (w%) of PAniNT in PMMA polymer matrix. Initially, PMMA was dissolved in excess amount of NMP and acetonitrile (volume ratio 2:8), and mixed with different wt% of PAniNT (0.15, 0.20, 0.25 and 0.30 wt%) by using ultrasonication. The ultrasonicated mixtures were then kept in an oven maintained at 35 °C for 6 h to get the PMMA/PAniNT polymer blends. These blends were then mixed with the liquid electrolyte, and kept for 24 h to get the PGEs. The liquid electrolyte was prepared by mixing 0.5 M LiI, 0.05 M I_2, 0.5 M TBP, 0.6 M MPI in a solvent mixture of NMP and acetonitrile (volume ratio 2:8). The as-prepared PGEs were later used for fabrication of the DSSSs. PGEs with 0, 0.15, 0.20, 0.25 and 0.30 wt% of PAniNT in it were designated as PGE(0), PGE(0.15), PGE(0.20), PGE(0.25) and PGE(0.30) respectively.

2.2.5 Assembling of the DSSCs

FTO coated glass sheets were sonicated for 30 min in a detergent solution followed by 30 min sonication in distilled water. The sheets were again sonicated for 30 min each in acetone and isopropanol to clean them properly and finally dried in N_2 environment. For preparation of the photoanodes, $TiCl_4$ (40 mM) treatment was done for 30 min at 70°C. It was followed by sintering at 400°C for 30 min for better contact between the FTO coated glass and TiO_2. Using doctoral blade technique, TiO_2 nanoparticle paste in ethanol was deposited on the $TiCl_4$ pretreated layer (thickness of ~20 µm). These films were dried at room temperature and then sintered at 450°C

for 30 min. Then the TiO_2 coated glass sheets were cooled down to room temperature followed by immersion in 0.3 mM of N719 dye prepared in acetonitrile/ethanol (volume ratio 1:1) solvent mixture for 24 h. Finally, the dye adsorbed TiO_2 coated glass sheets were cleaned with absolute ethanol and dried in a moisture-free environment, and used as photoanodes. To prepare the Pt counter electrodes, 7 mM H_2PtCl_6 solution in isopropanol was prepared. Spin coating technique was used to apply the H_2PtCl_6 solution onto the cleaned conductive FTO coated glass sheets. Then the glass sheets were heated at 400°C for 30 min for better interfacial properties followed by immersion in an aqueous solution of $NaBH_4$ (60 mM) [31].

Finally, a series of DSSCs with different wt% of PAniNT were fabricated by placing the as-prepared gel electrolytes between a dye adsorbed TiO_2 photoanode and a Pt counter electrode, using 25 µm thick Solaronix thermal polymer spacers. The gap between the two electrodes was completely filled by placing the required amount of gel electrolyte. The fabricated prototype devices were kept at 60°C for 5 min to improve the interfacial contact between gel electrolyte and dye adsorbed TiO_2 layer [32–34].

2.2.6 Characterization

A Nicolet Impact-410 IR spectrometer was used to record the Fourier transform infrared (FTIR) spectra of the prepared samples by using potassium bromide (KBr) pellet in the range of 400–4000 cm^{-1} at room temperature. Morphological studies of the PGEs were carried out using a Jeol-JSM-6390 LV scanning electron microscope (SEM). A solar simulator with xenon arc lamp with irradiation of 100 mW cm^{-2} and AM 1.5 was used to provide 1 sun illumination. The *J-V* characteristic plots were recorded under illumination of 100 mW cm^{-2} xenon arc lamp in ambient atmosphere by applying a potential sweep to the DSSCs. Then, the fill factors (*FF*) and light-to-electric conversion efficiencies (η) were calculated from these plots using **Eqs. (1.9)** and **(1.10)** described in Chapter 1 [35]. HIOKI IM3570 electrochemical impedance workstation was used to explore the electrochemical impedance spectroscopy (EIS) data. EIS was measured under illumination to investigate the quality of the DSSCs, with frequency range from 1 MHz to 0.1 Hz at an amplitude of 10 mV. Z-view software was used for fitting and analyzing the obtained spectra. The temperature dependence of the ionic conductivities was examined from EIS measurements by sandwiching the gel electrolytes between two stainless steel electrodes with space gap (25 µm) from 25°C to 60°C. The ionic conductivity was calculated by using **Eq. (2.1)**.

$$\sigma = L / AR_b \quad \text{(2.1)}$$

where L, A and R_b are the thickness, surface area and bulk resistance of the PGEs respectively.

2.3 Results and discussion

2.3.1 Structural analysis (FTIR spectra)

Figure 2.1 shows the FTIR spectra of PMMA, PAniNT and PMMA/PAniNT polymer blends. Absorption peaks at around 2940 cm^{-1} and 1460 cm^{-1} are observed in the FTIR spectrum of PMMA (**Figure 2.1(a)** due to C-H stretching and bending vibrations respectively. Strong peaks at 1729 cm^{-1} and 1149 cm^{-1} appear due to stretching vibrations of C=O and C-O bonds present in the ester group of PMMA. These functional groups play a significant role in the formation of gel electrolytes. The peak at 987 cm^{-1} is the characteristic peak for PMMA. The broad peak at 3446 cm^{-1} is due to the O-H group of water molecules adsorbed on PMMA polymer matrix. In the FTIR spectrum of PAniNT, (**Figure 2.1(b)**) peaks at around 3433 cm^{-1} and 1600 cm^{-1} are observed due to N-H stretching and bending vibrations respectively. A few peaks around 1478 cm^{-1} appear due to C=C stretching vibrations present in the aromatic rings. The peak at 1291 cm^{-1} is responsible for the C-N stretching vibrations in PAniNT [36]. From the FTIR spectrum of PMMA/PAniNT blend with 0.30 wt% of PAniNT (**Figure 2.1(c)**), it is evident that two individual polymers endeavor to

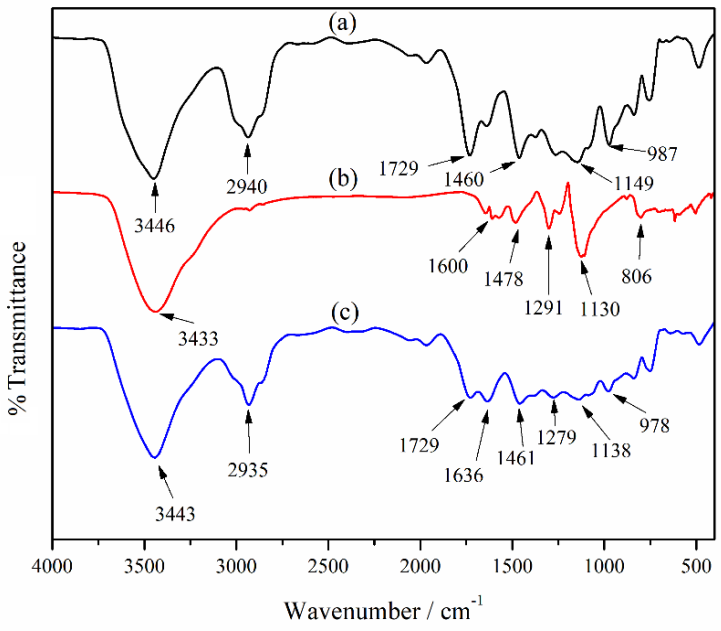

Figure 2.1. Characteristic FTIR absorption spectra of **(a)** PMMA, **(b)** PAniNT and **(c)** PMMA/PAniNT polymer blend with 0.30 wt% of PAniNT.

reserve their functional identity in the polymer blend although some bond vibrations are slightly affected. Shifting of the peaks areas are due to the interaction between the lone pair on nitrogen of PAniNT and electron deficient carbon center of PMMA. Peaks at 1729 cm^{-1}, 3443 cm^{-1} and 1636 cm^{-1} may appear respectively because of the stretching vibrations of C=O and stretching

and bending vibrations of N-H present in the polymer blend. The peaks around 1461 cm^{-1} and 1131 cm^{-1} are due to stretching vibration of C=C double bonds and bending vibrations of C-O bonds respectively. The attractive interactions between the functional groups of the solvent molecules and the functional groups present in the polymer blend help to trap the liquid electrolyte considerably.

2.3.2 Morphological analysis

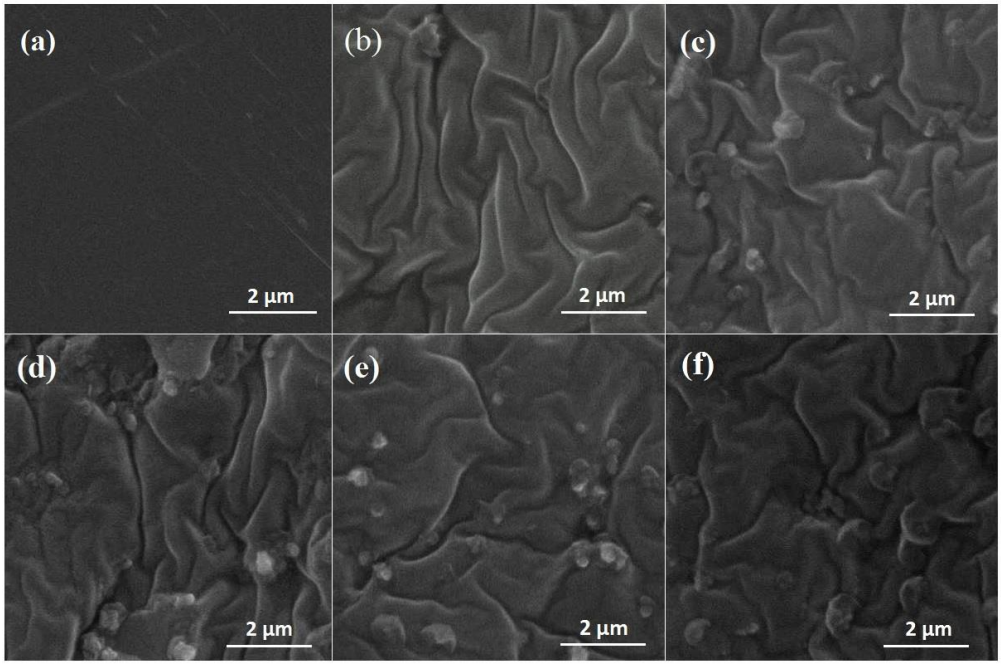

Figure 2.2. SEM images of **(a)** PMMA/PAniNT polymer blend with 0.30% of PAniNT without electrolyte, and PMMA/PAniNT based PGEs with **(b)** 0 wt%, **(c)** 0.15 wt%, **(d)** 0.20 wt%, **(e)** 0.25 wt% and **(f)** 0.30 wt% of PAniNT.

SEM was used to investigate the surface morphology of different PMMA/PAniNT based gel electrolytes (**Figure 2.2**). A ~25 µm thick coating of the PGEs were used to carry out the SEM analysis. **Figure 2.2(a)** shows the SEM micrograph of the PMMA/PAniNT polymer blend with 0.30 wt% of PAniNT without the liquid electrolyte. The image shows a smooth surface. **Figure 2.2((b)-(f))** represent the surface morphologies of the gel electrolytes with different wt% of PAniNT. The surface becomes wavy due to the absorption of the liquid electrolyte. However, there is not any noticeable change of surface morphology with varying wt% of PAniNT.

2.3.3 Photovoltaic performances

Figure 2.3 shows the *J-V* characteristics of the DSSCs employing different wt% of PAniNT in the PMMA/PAniNT polymer blend based PGEs measured under irradiation. The photovoltaic parameters of the DSSCs are summarized in **Table 2.1**.

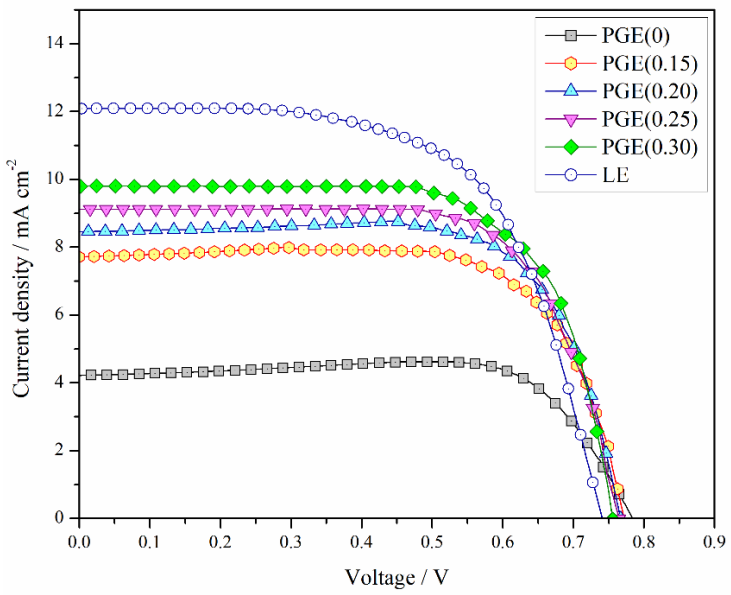

Figure 2.3. *J-V* characteristics of various DSSCs employing liquid electrolyte and PGEs with different wt% of PAniNT in the PMMA/PAniNT polymer blend.

Table 2.1. Photovoltaic parameters of the DSSCs employing liquid electrolyte and different PGEs

	LE*	**Polymer gel electrolyte**				
		PGE(0)**	PGE(0.15)**	PGE(0.20)**	PGE(0.25)**	PGE(0.30)**
V_{OC} / V	0.737	0.785	0.769	0.767	0.765	0.756
J_{SC} / mA cm^{-2}	12.09	4.23	7.71	8.45	9.12	9.80
FF	0.63	0.78	0.72	0.72	0.70	0.68
η / %	5.66	2.58	4.27	4.67	4.88	5.11

* LE stands for liquid electrolyte.

** PGE stands for polymer gel electrolyte and the number within bracket represents the wt% of added PAniNT in the gel electrolyte.

The amount of PAniNT in PMMA anchors the values of V_{OC} and J_{SC}. The gel electrolyte without PAniNT in PMMA shows J_{SC} value of 4.23 mA cm^{-2}. The incorporation of PAniNT leads to a gradual improvement in J_{SC} and the efficiency of the device. The highest J_{SC} value of 9.80 mA cm^{-2} is obtained with 0.30 wt% PAniNT. This is due to the increase in ionic conductivities of the PGEs with the addition of PAniNT. This effect is presently discussed.

2.3.4 Ionic conductivity analysis

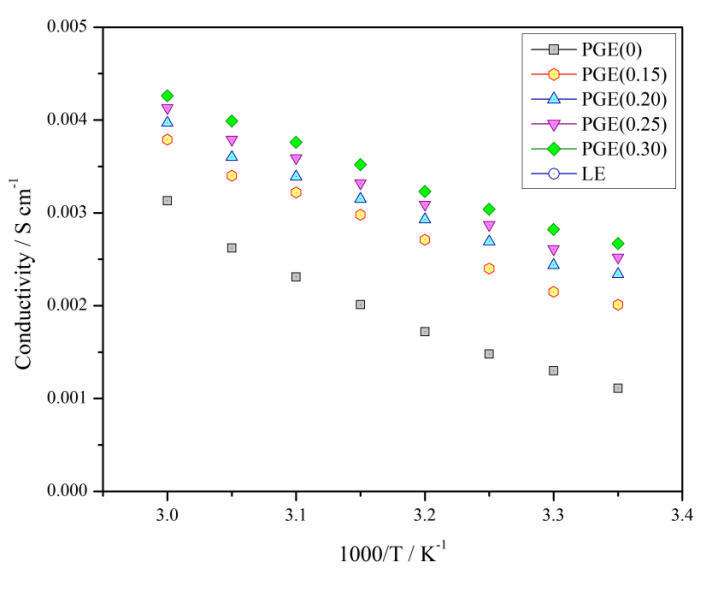

Figure 2.4. Temperature dependence of ionic conductivities of the PGEs with different wt% of PAniNT in PMMA/PAniNT PGE under applied bias potential of 0.75 V.

To investigate the ionic transport behavior in the PGEs, their ionic conductivities at different temperatures were measured from EIS by sandwiching the PGEs in between two steel electrodes without irradiation under a bias potential of 0.75 V. The bias potential was set at 0.75 V as the V_{OC} values of the fabricated DSSCs were found near this potential. The thickness of the coating of PGEs was 25 µm as a space gap with 25 µm was used between the two stainless steel electrodes. **Figure 2.4** exhibits the Arrhenius behavior which can be fitted with **Eq. (2.2)**.

$$\sigma = A\exp(-E_A / RT) \quad \text{(2.2)}$$

where σ, E_A, R and T represent ionic conductivity, activation energy, universal gas constant and temperature respectively.

The addition of PAniNT in PMMA gel electrolyte enhances the ionic conductivity, as well as the viscosity of the gel electrolyte. This gel electrolyte is not a free-flowing liquid, but moves only under pressure between the two electrodes. Thus it behaves like a good ionic transport medium for facilitating physical diffusion of I_3^- ions. The activation energy of the PGE decreases with the increase in amount of PAniNT in PMMA. The calculated activation energies at room temperature are 24.63, 14.96, 12.58, 11.64 and 11.16 kJ mol^{-1} for PGE(0), PGE(0.15), PGE(0.20), PGE(0.25) and PGE(0.30) respectively. The lower activation energy is helpful in increasing the J_{SC} values of the DSSCs [42].

2.3.5 Electrochemical impedance analysis

To elucidate the effect of the PGE on the charge transfer process, EIS data were recorded under irradiation of light. Three semicircles are seen in the Nyquist plot (Z' vs $-Z''$) as shown in **Figure 2.5**.

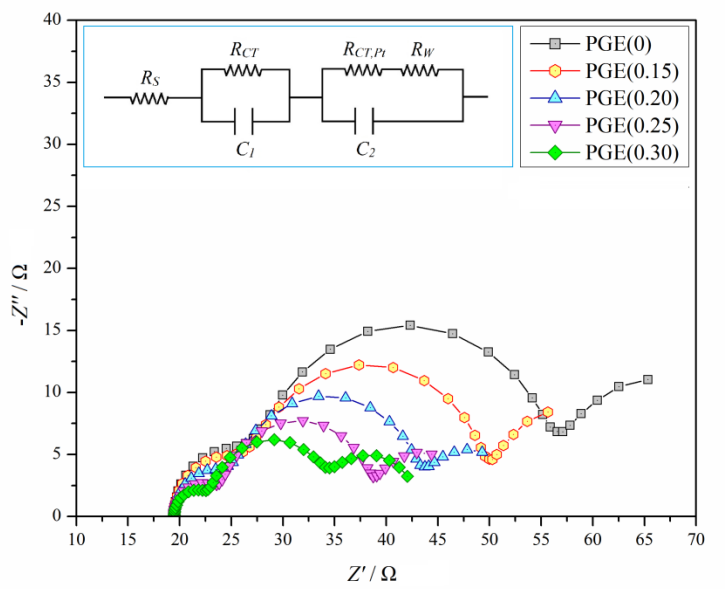

Figure 2.5. Nyquist plots of the DSSCs employing liquid electrolyte and PGEs with different PAniNT content obtained under irradiation. The inset shows the corresponding equivalent circuit model.

Table 2.2. EIS parameters of the DSSCs employing liquid electrolyte and different PGEs under irradiation.

	LE*	**Polymer gel electrolyte**				
		PGE(0)**	PGE(0.15)**	PGE(0.20)**	PGE(0.25)**	PGE(0.30)**
$R_{CT,Pt}$ / Ω	1.45	7.87	7.21	5.61	4.53	3.43
R_{CT} / Ω	7.24	29.21	23.32	18.45	16.21	11.40

* LE stands for liquid electrolyte.

** PGE stands for polymer gel electrolyte and the number within bracket represents the wt% of added PAniNT in the gel electrolyte.

The charge transfer at the Pt counter electrode ($R_{CT,Pt}$) is represented by the high frequency range, the charge transfer at the photoanode/electrolyte interface (R_{CT}) is assigned by the middle range and the ionic diffusion in electrolyte is characterized by the low frequency range of the

Nyquist plot. On the basis of the transmission line model, the EIS data are fitted with an equivalent circuit (shown in inset in the **Figure 2.5**) to investigate the charge transfer processes [43,44]. Both the charge transfer resistances are given in **Table 2.2**. The PGEs exhibit higher R_{CT} values as compared to that of the liquid electrolyte. This might be due to less interfacial charge recombination at the photoanode. However, this resistance decreases with the increment of PAniNT in the PGEs. This is an indication of the positive effect of PAniNT on the charge transfer process at the photoanode.

To further clarify the effect of the PGEs on the charge transfer process at the platinum counter electrode, the first semicircle of the Nyquist plot for electrolytes is considered. The $R_{CT,Pt}$ value for the liquid electrolyte is lower than that of the PGEs (**Table 2.2**). At the Pt counter electrode, the I_3^- ions get reduced to I^- ions by consuming the electrons coming from the external circuit through charge transfer reactions. Thus, this charge transfer process at the electrolyte/Pt counter electrode anchors the magnitude of $R_{CT,Pt}$. The higher availability of I_3^- ions at the Pt counter electrode enhances the charge transfer process. Many parameters determine the availability of I_3^- ions at the Pt counter electrode: the concentration and diffusion of I_3^- ions are the two most important parameters [45]. The polymer network in gel electrolyte hinders the diffusion process resulting in higher $R_{CT,Pt}$. The PGE without PAniNT shows a higher $R_{CT,Pt}$ value of 7.87 Ω. The addition of PAniNT in the gel electrolyte lowers the magnitude of $R_{CT,Pt.}$ This is due to the better diffusion process and increased ionic conductivity with the incorporation of PAniNT in the gel electrolyte. But higher wt% of PAniNT (>0.30 wt%) in PMMA damages the cell performance due to agglomeration of PAniNT.

2.3.6 Long-term stability

To study the durability of the DSSCs employing liquid electrolyte and PGEs, the values of V_{OC} and J_{SC} were recorded using *J-V* characteristics for the DSSCs for duration of 1000 h at room temperature. The results are shown in **Figure 2.6(a)** and **(b)**. The durability of the DSSCs employing PGEs improves significantly as the solvent molecules are trapped in the polymer matrix. PGE(0) exhibits similar J_{SC} values (4.223 mA cm^{-2}) even after 1000 h of testing. PGE(0.15), PGE(0.20), PGE(0.25) and PGE(0.30) show noticeable retention of the J_{SC} values from 200 h to 600 h of testing. After 1000 h, though, these values decrease from their initial values of 7.71, 8.45, 9.12 and 9.80 mA cm^{-2} to 5.86, 5.27, 5.01 and 4.67 mA cm^{-2}, respectively. PGE(0.30) with PCE of 5.11% shows 47.6% retention of the J_{SC} value. The DSSC fabricated with the liquid electrolyte does not even show any current after just 200 h of testing. It can be easily concluded that the DSSCs fabricated with PGEs exhibit good stability compared to the DSSC devised with liquid electrolyte. DSSCs employing different gel electrolytes exhibit almost

similar V_{OC} values as shown in **Figure 2.6(b)**. Thus, PGEs encumber the volatilization process of solvents, improving the durability and reliability of the DSSCs. Also, the optimization of ionic conductivity with conducting polymer like PAniNT leads to exhibition of high performing DSSCs.

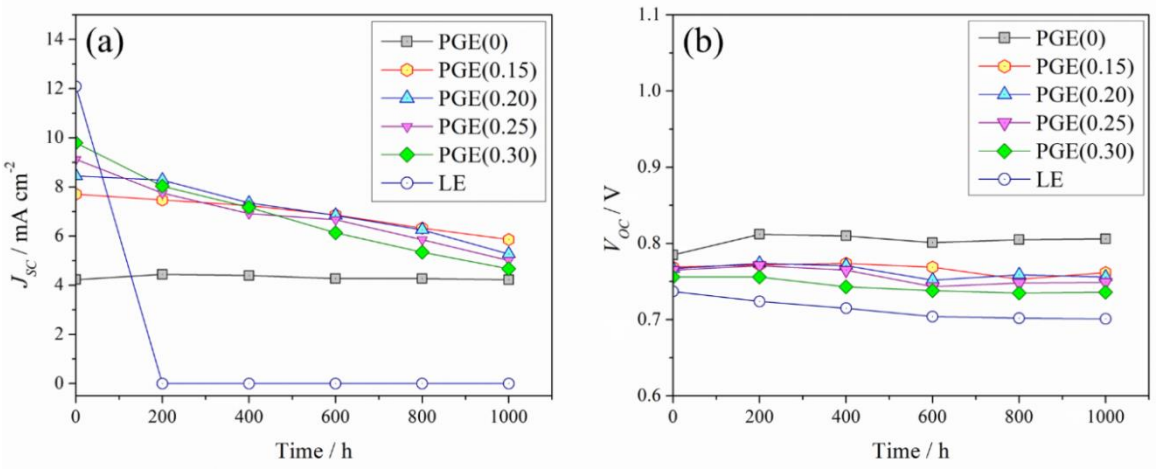

Figure 2.6. (a) J_{SC} and **(b)** V_{OC} values for different DSSCs with PGEs and liquid electrolyte for upto 1000 h of testing.

2.4 Conclusion

- A gel electrolyte based on PMMA polymer host was synthesized by incorporating different amounts (in weight percent, wt%) of PAniNT in the polymer matrix. Successful formation of the PGEs were verified from their structural and morphological characterizations.
- An optimized DSSC device fabricated with PGE containing 0.30 wt% PAniNT exhibited the highest efficiency of 5.11% under simulated light with illumination of 100 mW cm^{-2} (AM 1.5). The short-circuit current density (J_{SC}), open-circuit voltage (V_{OC}) and fill factor (FF) values of the cell were 9.80 mA cm^{-2}, 0.756 V and 0.68 respectively.
- The ionic conductivities of the PGEs were calculated from their electrochemical impedance spectroscopy (EIS) data. An increase in the values of ionic conductivity was seen with the increment of PAniNT in the PGEs.
- The charge transfer resistances at the photoanode/PGE interface (R_{CT}), and at the counter electrode/PGE interface ($R_{CT,Pt}$) were computed from the EIS data. The PGE with 0.30 wt% PAniNT showed R_{CT} value of 11.40 Ω and $R_{CT,Pt}$ value of 3.43 Ω.
- The quasi-solid-state DSSC showed significant long-term stability in comparison to the DSSC prepared with liquid electrolyte. The PGE with 0.30 wt% PAniNT retained 47.6% of the J_{SC} value after 1000 h of testing.

2.5 References

[1] O'Regan, B. and Grätzel, M. A low-cost, high-efficiency solar cell based on dye-sensitized colloidal TiO_2 films. *Nature*, 353(6346):737-740, 1991.

[2] Bach, U., Lupo, D., Comte, P., Moser, J. E., Weissörtel, F., Salbeck, J., Spreitzer, H., and Grätzel, M. Solid-state dye-sensitized mesoporous TiO_2 solar cells with high photon-to-electron conversion efficiencies. *Nature*, 395(6702):583-585, 1998.

[3] Grätzel, M. Photoelectrochemical cells. *Nature*, 414(6861):338-344, 2001.

[4] Grätzel, M. Perspectives for dye-sensitized nanocrystalline solar cells. *Progress in Photovoltaics: Research and Applications*, 8(1):171-185, 2000.

[5] Nasr, C., Hotchandani, S., and Kamat, P. V. Role of iodide in photoelectrochemical solar cells. electron transfer between iodide ions and ruthenium polypyridyl complex anchored on nanocrystalline SiO_2 and SnO_2 films. *The Journal of Physical Chemistry B*, 102(25):4944-4951, 1998.

[6] Kebede, Z. and Lindquist, S.-E. Donor–acceptor interaction between non-aqueous solvents and I_2 to generate I_3^-, and its implication in dye sensitized solar cells. *Solar Energy Materials and Solar Cells*, 57(3):259-275, 1999.

[7] Durrant, J. R. and Haque, S. A. Solar cells: A solid compromise. *Nature materials*, 2(6):362-363, 2003.

[8] Han, H. W., Liu, W., Zhang, J., and Zhao, X. Z. A hybrid poly(ethylene oxide)/poly(vinylidene fluoride)/TiO_2 nanoparticle solid-state redox electrolyte for dye-sensitized nanocrystalline solar cells. *Advanced Functional Materials*, 15(12):1940-1944, 2005.

[9] Bach, U., Lupo, D., Comte, P., Moser, J. E., Weissörtel, F., Salbeck, J., Spreitzer, H., and Grätzel, M. Solid-state dye-sensitized mesoporous TiO_2 solar cells with high photon-to-electron conversion efficiencies. *Nature*, 398:583-585, 1998.

[10] Snaith, H. J. and Schmidt-Mende, L. Advances in liquid-electrolyte and solid-state dye-sensitized solar cells. *Advanced Materials*, 19(20):3187-3200, 2007.

[11] Fabregat-Santiago, F., Bisquert, J., Cevey, L., Chen, P., Wang, M., Zakeeruddin, S. M., and Grätzel, M. Electron transport and recombination in solid-state dye solar cell with spiro-OMeTAD as hole conductor. *Journal of the American Chemical Society*, 131(2):558-562, 2009.

[12] Zakeeruddin, S. M. and Grätzel, M. Solvent-free ionic liquid electrolytes for mesoscopic dye-sensitized solar cells. *Advanced Functional Materials*, 19(14):2187-2202, 2009.

[13] de Freitas, J. N., Nogueira, A. F., and De Paoli, M. A. New insights into dye-sensitized solar cells with polymer electrolytes. *Journal of Materials Chemistry*, 19(30):5279,

2009.

[14] Wang, Y. Recent research progress on polymer electrolytes for dye-sensitized solar cells. *Solar Energy Materials and Solar Cells*, 93(8):1167-1175, 2009.

[15] Wu, J. H., Lan, Z., Lin, J. M., Huang, M. L., Hao, S. C., Sato, T., and Yin, S. A novel thermosetting gel electrolyte for stable quasi-solid-state dye-sensitized solar cells. *Advanced Materials*, 19(22):4006-4011, 2007.

[16] Chen, C. L., Teng, H., and Lee, Y. L. In situ gelation of electrolytes for highly efficient gel-state dye-sensitized solar cells. *Advanced Materials*, 23(36):4199-4204, 2011.

[17] Cao, F., Oskam, G., and Searson, P. C. A solid state dye sensitized photoelectrochemical cell. *The Journal of Physical Chemistry*, 99(47):17071-17073, 1995.

[18] Yang, Y., Zhou, C.H., Xu, S., Hu, H., Chen, B. L., Zhang, J., Wu, S. J., Liu, W., and Zhao, X. Z. Improved stability of quasi-solid-state dye-sensitized solar cell based on poly (ethylene oxide)–poly (vinylidene fluoride) polymer-blend electrolytes. *Journal of Power Sources*, 185(2):1492-1498, 2008.

[19] Wang, G., Zhou, X., Li, M., Zhang, J., Kang, J., Lin, Y., Fang, S., and Xiao, X. Gel polymer electrolytes based on polyacrylonitrile and a novel quaternary ammonium salt for dye-sensitized solar cells. *Materials Research Bulletin*, 39(13):2113-2118, 2004.

[20] Tu, C. W., Liu, K. Y., Chien, A. T., Lee, C. H., Ho, K. C., and Lin, K. F. Performance of gelled-type dye-sensitized solar cells associated with glass transition temperature of the gelatinizing polymers. *European Polymer Journal*, 44(3):608-614, 2008.

[21] Wang, P., Zakeeruddin, S. M., Moser, J. E., Nazeeruddin, M. K., Sekiguchi, T., and Grätzel, M. A stable quasi-solid-state dye-sensitized solar cell with an amphiphilic ruthenium sensitizer and polymer gel electrolyte. *Nature Materials*, 2(6):402-407, 2003.

[22] Wang, P., Zakeeruddin, S. M., Exnar, I., and Grätzel, M. High efficiency dye-sensitized nanocrystalline solar cells based on ionic liquid polymer gel electrolyte. *Chemical Communications*, 8(24):2972-2973, 2002.

[23] Wu, J. H., Hao, S. C., Lan, Z., Lin, J. M., Huang, M. L., Huang, Y. F., Fang, L. Q., Yin, S., and Sato, T. A thermoplastic gel electrolyte for stable quasi-solid-state dye-sensitized solar cells. *Advanced Functional Materials*, 17(15):2645-2652, 2007.

[24] Wu, J., Li, P., Hao, S., Yang, H., and Lan, Z. A polyblend electrolyte (PVP/PEG+ KI+ I_2) for dye-sensitized nanocrystalline TiO_2 solar cells. *Electrochimica Acta*,

[25] Hsu, Y.-C., Tseng, L.-C., and Lee, R.-H. Graphene oxide sheet-polyaniline nanohybrids for enhanced photovoltaic performance of dye-sensitized solar cells. *Journal of Polymer Science Part B: Polymer Physics*, 52(4):321-332, 2014.

[26] Aram, E., Ehsani, M., and Khonakdar, H. A. Improvement of ionic conductivity and

performance of quasi-solid-state dye sensitized solar cell using PEO/PMMA gel electrolyte. *Thermochimica Acta*, 615:61-67, 2015.

[27] Chen, C.-L., Teng, H., and Lee, Y.-L. Preparation of highly efficient gel-state dye-sensitized solar cells using polymer gel electrolytes based on poly(acrylonitrile-co-vinyl acetate). *Journal of Materials Chemistry*, 21(3):628-632, 2011.

[28] Ou, R., Gupta, S., Parker, C. A., and Gerhardt, R. A. Fabrication and electrical conductivity of poly(methyl methacrylate) (PMMA)/carbon black (CB) composites: Comparison between an ordered carbon black nanowire-like segregated structure and a randomly dispersed carbon black nanostructure. *Journal of Physical Chemistry B*, 110(45):22365-22373, 2006.

[29] Araujo, P. L. B., Araujo, E. S., Santos, R. F. S., and Pacheco, A. P. L. Synthesis and morphological characterization of PMMA/polyaniline nanofiber composites. *Microelectronics Journal*, 36(11):1055-1057, 2005.

[30] Sim, B. and Choi, H. J. Facile synthesis of polyaniline nanotubes and their enhanced stimuli-response under electric fields. *RSC Advances*, 5(16):11905-11912, 2015.

[31] Sim, K., Sung, S. J., Jo, H. J., Jeon, D. H., Kim, D. H., and Kang, J. K. Electrochemical investigation of high-performance dye-sensitized solar cells based on molybdenum for preparation of counter electrode. *International Journal of Electrochemical Science*, 8:8272-8281, 2013.

[32] Miyamoto, T. and Shibayama, K. Free-volume model for ionic conductivity in polymers. *Journal of Applied Physics*, 44(12):5372-5376, 1973.

[33] Li, Q., Wu, J., Tang, Z., Xiao, Y., Huang, M., and Lin, J. Application of poly(acrylic acid-g-gelatin)/polypyrrole gel electrolyte in flexible quasi-solid-state dye-sensitized solar cell. *Electrochimica Acta*, 55:2777-2781, 2010.

[34] Lin, L. Y., Tsai, C. H., Wong, K. T., Huang, T. W., Hsieh, L., Liu, S. H., Lin, H. W., Wu, C. C., Chou, S. H., Chen, S. H., and Tsai, A. I. Organic dyes containing coplanar diphenyl-substituted dithienosilole core for efficient dye-sensitized solar cells. *Journal of Organic Chemistry*, 75(14):4778-4785, 2010.

[35] Yu, J., Fan, J., and Lv, K. Anatase TiO_2 nanosheets with exposed (001) facets: Improved photoelectric conversion efficiency in dye-sensitized solar cells. *Nanoscale*, 2(10):2144-2149, 2010.

[36] Liu, D., Wang, X., Deng, J., Zhou, C., Guo, J., and Liu, P. Crosslinked carbon nanotubes/polyaniline composites as a pseudocapacitive material with high cycling stability. *Nanomaterials*, 5(2):1034-1047, 2015.

[37] Ren, Y., Zhang, Z., Fang, S., Yang, M., and Cai, S. Application of PEO based gel

network polymer electrolytes in dye-sensitized photoelectrochemical cells. *Solar Energy Materials and Solar Cells*, 71(2):253-259, 2002.

[38] Kubo, W., Kitamura, T., Hanabusa, K., Wada, Y., and Yanagida, S. Quasi-solid-state dye-sensitised solar cells using room temperature molten salts and a low molecular weight gelator. *Chemical Communications*, 4:374-375, 2002.

[39] Mohmeyer, N., Wang, P., Schmidt, H. W., Zakeeruddin, S. M., and Grätzel, M. Quasi-solid-state dye sensitized solar cells with 1,3:2,4-di-O-benzylidene-D-sorbitol derivatives as low molecular weight organic gelators. *Journal of Materials Chemistry*, 14(12):1905-1909, 2004.

[40] Dong, R. X., Shen, S. Y., Chen, H. W., Wang, C. C., Shih, P. T., Liu, C. T., Vittal, R., Lin, J. J., and Ho, K. C. A novel polymer gel electrolyte for highly efficient dye-sensitized solar cells. *Journal of Materials Chemistry A*, 1(29):8471, 2013.

[41] Yuan, S., Tang, Q., He, B., and Yu, L. Conducting gel electrolytes with microporous structures for efficient quasi-solid-state dye-sensitized solar cells. *Journal of Power Sources*, 273:1148-1155, 2015.

[42] Huo, Z., Dai, S., Zhang, C., Kong, F., Fang, X., Guo, L., Liu, W., Hu, L., Pan, X., and Wang, K. Low molecular mass organogelator based gel electrolyte with effective charge transport property for long-term stable quasi-solid-state dye-sensitized solar cells. *Journal of Physical Chemistry B*, 112(41):12927-12933, 2008.

[43] Bisquert, J., Grätzel, M., Wang, Q., and Fabregat-Santiago, F. Three-channel transmission line impedance model for mesoscopic oxide electrodes functionalized with a conductive coating. *Journal of Physical Chemistry B*, 110(23):11284-11290, 2006.

[44] Bisquert, J. Theory of the impedance of electron diffusion and recombination in a thin layer. *Journal of Physical Chemistry B*, 106(2):325-333, 2002.

[45] Halme, J., Vahermaa, P., Miettunen, K., and Lund, P. Device physics of dye solar cells. *Advanced Materials*, 22(35):E210-E234, 2010.